1 **Title: Autophagic degradation of the Cucumber mosaic virus virulence factor 2b balances**

2 **antiviral RNA silencing with proviral plant fitness and virus seed transmission**

3

4

5 Short title: Autophagy in CMV disease

6

7 Authors;

8 Aayushi Shukla[¶], Gesa Hoffmann[¶], Silvia López-González, Daniel Hofius and Anders Hafrén*

9

10 Affiliations;

11 Department of Plant Biology, Uppsala BioCenter, Swedish University of Agricultural Sciences

12 and Linnean Center for Plant Biology, Box 7080, 75007 Uppsala, Sweden

13

14

15

16 *Corresponding author

17 Email: anders.hafren@slu.se

18

19

20 [¶]These authors contributed equally to this work.

21

Abstract

Autophagy is a conserved intracellular degradation pathway that has recently emerged as an integral part of plant responses to virus infection. The elucidated mechanisms of autophagy range from the selective degradation of viral components to a more general attenuation of disease symptoms. In addition, several viruses are able to manipulate the autophagy machinery and counteract autophagy-dependent resistance. Despite these findings, the complex interplay of autophagy activities, viral pathogenicity factors, and host defence pathways in disease development remains poorly understood. In the current study, we analysed the interaction between autophagy and Cucumber mosaic virus (CMV) in *Arabidopsis thaliana*. We show that autophagy is induced during CMV infection and promotes the turnover of the major CMV virulence protein and RNA silencing suppressor 2b. Intriguingly, 2b itself dampens plant autophagy. In accordance with 2b degradation, we found that autophagy provides resistance against CMV by reducing viral RNA accumulation in an RNA silencing-dependent manner. Moreover, autophagy and RNA silencing pathways contribute to plant longevity and fecundity of CMV infected plants in an additive manner, uncoupling it from resistance. In addition to reduced fecundity, autophagy-deficient plants also failed to support seed transmission of the virus. We propose that autophagy attenuates CMV virulence via 2b degradation and thereby increases both plant and virus fitness with a trade-off penalty arising from increased RNA silencing-mediated resistance.

Author summary

The capacity of plants to fight pathogenic viruses in order to survive and minimize damage relies on profound cellular reprogramming events. These include the synthesis of new as well as the degradation of pre-existing cellular components, together shifting cellular homeostasis

47   towards a better tolerance of disease and fortification of antiviral defence mechanisms.

48   Autophagy is a prominent and highly conserved cellular degradation pathway that supports

49   plant stress resilience. Autophagy functions vary broadly and range from rather unspecific

50   renewal of cytoplasm to highly selective degradation of a wide collection of specific substrates.

51   Autophagy is well established to be involved during virus infections in animals, and its

52   importance has also recently emerged in virus diseases of plants. However, we are still far from

53   a comprehensive understanding of the complexity of autophagy activities in host-virus

54   interactions and how autophagy pathway engineering could be applied against viruses. Here,

55   we have analyzed one of the traditional model plant viruses, Cucumber mosaic virus (CMV),

56   and its interactions with autophagy. Our study revealed that autophagy is tightly integrated into

57   CMV disease, influencing processes from plant health to CMV epidemiology.

58

Introduction

59

60   Autophagy is a conserved eukaryotic mechanism that is important for cellular homeostasis

61   through its functions as a major catabolic system. In its simplest form, the autophagy process

62   is considered to sequester cytoplasmic portions non-selectively within a vesicular structure

63   called the autophagosome, which subsequently enters the lytic vacuole of plants for degradation

64   and recycling of nutrients. However, the extent to which autophagy operates in a non-selective

65   manner still remains an open question. In parallel, the examples of selective targeting of

66   autophagic substrates by specialized cargo receptors continues to increase (1, 2). The plant

67   autophagic molecular machinery was initially characterized in *Arabidopsis thaliana* and

68   subsequently recognised in algae, gymnosperms and other angiosperms (3). Core components

69   of this pathway include numerous ATG genes, such as ATG5, ATG7 and ATG8. Selective

70   autophagy is known to take part in the turn-over of substrates including chloroplasts,

71   peroxisomes, aggregates, ribosomes and proteasomes in plants. Selectivity opens the possibility

72   for several highly distinct autophagic processes to operate in parallel, and outlines the important

73   challenge to dissect the overall autophagy effect into its finer mechanisms.

74   Autophagy is induced by numerous environmental conditions, including abiotic stress

75   and nutrient limitation. Its importance for plant adaptation is established in part by the increased

76   sensitivity of autophagy-deficient plants to these conditions (3, 4). Autophagy also plays

77   important roles in plant-pathogen interactions including diseases caused by viruses, bacteria,

78   fungi and oomycetes (5). These studies support the notion that autophagy is a complex process

79   with several functions operating in parallel to influence the infection outcome. Because

80   pathogens commonly cause severe stress to their host plants, it is not surprising that infected

81   plants show an upregulation of autophagy upon infection (6-10). This finding outlines the

82   important concept that the interaction between pathogens and their hosts likely co-evolves in

83   the presence of an activated autophagy response. As a consequence, both pathogen and host

84   could try to utilize the plant autophagy process for their own benefit.

85   In virus-plant interactions, we can distinguish between two mechanisms that limit

86   disease. Host resistance refers to the ability to suppress virus multiplication whereas tolerance

87   is defined as the ability of the plant to minimise the infection-associated damage as a result of

88   the pathogen infection. Co-adaptation of hosts and viruses has resulted in a range of interactions

89   between antiviral resistance mechanisms and viral counter-strategies, together balancing plant

90   and virus fitness (11). Autophagy has been established as a prominent response pathway to

91   several viral infections in the animal field (12). An emerging theme from these studies is that

92   viruses have acquired properties to modify autophagy in many ways, including induction,

93   suppression and subversion of its functions. Evolution of such viral properties can be

94   considered to directly reflect the importance of autophagy for virus infection. Recently,

95   fundamental roles for autophagy have been identified in plant viral diseases, including

96   autophagic degradation of viral components, virus-based counteraction and modulation of

97   autophagy, as well as autophagy-mediated promotion of plant tolerance (7-9, 13, 14).

98   Interestingly, a connection between autophagy and the foremost antiviral defence pathway in

99   plants, RNA silencing, is emerging. Initially, autophagy was suggested to degrade the RNA

100   silencing suppressors of potyviruses (HCpro) and cucumoviruses (2b) (15), and we could

101   recently show that the autophagy cargo receptor NBR1 degrades HCpro to reduce virus

102   susceptibility and accumulation (7). Additionally, autophagy degrades the satellite ßC1 RNA

103   silencing suppressor of geminiviruses, AGO1 when targeted by the poleroviral RNA silencing

104   suppressor P0, and SGS3/RDR6 in the presence of potyviral VPg (9, 16, 17). Notably,

105   autophagy-based resistance was uncoupled from autophagy-based tolerance against a *Potyvirus*

106   (Turnip mosaic virus; TuMV) and a *Caulimovirus* (Cauliflower mosaic virus; CaMV) (7, 8).

107   Thus, autophagy shows complex interactions and a general potential for regulating plant virus

108   disease.

109   In this study we show that autophagy is induced during infection by Cucumber mosaic

110   virus (CMV; genus *Cucumovirus*), a positive-stranded RNA virus. We found that the viral RNA

111   silencing protein 2b has a modest capacity to dampen autophagy and is itself subject to

112   autophagic degradation. Because autophagy suppressed CMV RNA accumulation in an RNA

113   silencing- and AGO1-dependent manner, we propose that 2b degradation represents a

114   resistance mechanism that sensitizes CMV to RNA silencing. In a broader context, autophagy

115   and RNA silencing appear beneficial for CMV infection through synergistic promotion of plant

116   longevity, fecundity and viral seed transmission. Our results thereby reveal that autophagy

117   provides resistance by reducing virus accumulation as well as tolerance by decreasing disease

118   severity during CMV infection, and both processes seem to be linked to the autophagic

119   degradation of the major virulence factor 2b.

120

121   **Results**

122   **Autophagy suppresses disease severity and CMV accumulation**

123   A potential aspect influencing virus and plant fitness is the severity of disease. Previously, we

124   showed that biomass loss, as a measure for disease, was severely increased in loss-of-function

125   mutants of the core autophagy gene ATG5 but not in plants lacking the autophagy cargo

126   receptor NBR1 when infected with TuMV or CaMV (7, 8). In this study, we analysed whether

127   CMV-infected plants showed a similar dependence on functional autophagy by infecting WT,

128   *atg5* and *nbr1* plants with CMV and scoring disease symptoms at 28 days after infection (DAI).

129   While infected WT and *nbr1* plants appeared indistinguishable (Fig 1A) and showed a similar

130   loss in fresh weight (Fig 1B), infected *atg5* plants were severely dwarfed and showed a higher

131   fresh weight loss. We conclude that the core autophagy machinery, but not NBR1 is important

6

132   for the plant to attenuate CMV disease. This observation is similar to previous findings for

133   TuMV and CaMV (7, 8), and supports a universal role for autophagy in reducing disease

134   symptoms of pathogenic plant viruses.

135   Next, we determined CMV multiplication in WT, *atg5* and *nbr1* plants at 14 DAI (Fig

136   1C). Viral RNA accumulated to higher levels in *atg5* compared to WT and *nbr1* plants. Notably,

137   autophagy-dependent suppression of CMV RNA accumulation was NBR1-independent,

138   distinguishing it from selective autophagy pathways contributing to resistance against CaMV

139   and TuMV (7, 8). We could also detect higher levels of the viral 2b protein in *atg5* compared

140   to WT and *nbr1* plants by Western blotting (Fig 1D), further supporting that autophagy limits

141   CMV accumulation independently of NBR1. We further estimated virus susceptibility by

142   calculating the number of plants showing infection symptoms after mechanical sap inoculation

143   of CMV, and found that infection rate was increased in autophagy-deficient *atg7* mutants

144   compared to WT plants (Fig 1E). Together, these results establish autophagy as a suppressor of

145   CMV infection by decreasing susceptibility, viral RNA accumulation and disease

146   symptomology.

147

148   **Autophagy is induced during CMV infection**

149   Owing to the effect of autophagy in CMV infection (Fig 1), we set out to determine whether

150   autophagy levels were altered during infection. We used an Arabidopsis line that stably

151   expresses GFP-ATG8a, which is a commonly applied marker for detection of autophagosomes.

152   Distribution of this marker was altered in CMV infected tissue, including increased numbers of

153   smaller GFP-ATG8a puncta that likely represented autophagosomes (Fig 2A and B). Infected

154   tissue also contained larger GFP-ATG8a labelled structures that were not observed in healthy

155   tissue. Treatment with concanamycin A (conA), an inhibitor of the vacuolar ATPase, was used

156   to stabilize autophagic bodies delivered into the vacuole (8). The number of GFP-ATGA8a

7

157   puncta substantially increased upon conA application in infected tissue (Fig 2A and B),

158   suggesting that autophagy is both activated and completed during CMV infection.

159   The processing of free GFP from the GFP-ATG8 fusion protein is regarded as another

160   proxy for autophagy flux in plants. Free GFP levels were higher in CMV infected tissue

161   compared to the healthy control (Fig 2C), supporting elevated autophagy levels. Moreover, we

162   observed higher transcript levels of autophagy-related genes *ATG8a*, *ATG8e* and *NBR1* in CMV

163   infected tissue (Fig 2D), suggesting transcriptional activation of autophagy. NBR1 delivers

164   cargo to autophagosomes and gets degraded in the process, making the NBR1 protein to mRNA

165   ratio another indicator of autophagy activity and flux. Notably, despite elevated *NBR1* transcript

166   levels, there was only slight increase in NBR1 protein accumulation (Fig 2E), suggesting

167   enhanced autophagic degradation during CMV infection. These assays together indicated that

168   autophagy is induced and functional during CMV infection.

169

170   **CMV 2b protein modulates the autophagy response**

171   Our observation of infection-induced autophagy together with the autophagy-dependent

172   suppression of viral RNA accumulation and disease severity prompted us to analyse whether

173   individual CMV proteins could modulate autophagy. First, we used a recently developed

174   quantitative assay in *Nicotiana benthamiana* leaves, that is based on the transient expression of

175   ATG8a fused to *Renilla* luciferase (RLUC) together with firefly luciferase (FLUC) as internal

176   control (6). Co-expression of the viral protein 2b substantially increased RLUC-ATG8a

177   accumulation in relation to FLUC, while 2a, 3a and CP behaved similar as the GUS control

178   (Fig 3A). This result identified 2b as a potential suppressor of autophagy, and as none of the

179   viral proteins seemed to recapitulate infection-induced autophagy on their own, this elevation

180   is likely to be a result of the full infection process. Over-expression of ATG3 was previously

181   shown to induce autophagy in *N. benthamiana* (18) and indeed resulted in a 5-fold increase of

8

182   FLUC to RLUC-ATG8a ratio (Fig 3B). Additional expression of 2b diminished the inducing

183   effect by ATG3, further supporting the autophagy-suppressing activity of 2b in this system.

184   Importantly, we also found that autophagy was modestly down-regulated in 2b

185   transgenic Arabidopsis seedlings as indicated by a reduced number of GFP-ATG8a labelled

186   autophagosomes in conA treated seedling roots (Fig 3C) and a decreased accumulation of free

187   GFP from GFP-ATG8a (Fig 3D). 2b is the major pathogenicity factor of CMV and 2b

188   transgenic plants show severe growth retardation as well as different morphological

189   abnormalities (19) (Fig 3E). However, the transcript levels for *ATG8a*, *ATG8e* and *NBR1*

190   remained unaffected in 2b transgenic plants (Fig 3F). Thus, the 2b-mediated dampening of

191   autophagy levels appear to occur post-transcriptionally and, 2b pathogenicity alone is not

192   causative for the up-regulation of autophagy pathway transcripts during CMV infection (Fig

193   2D). We therefore conclude that 2b is capable of attenuating the autophagy response.

194

195   **CMV 2b is degraded through autophagy**

196   Previously, autophagy-dependent 2b degradation has been proposed based on its accumulation

197   in response to the PI3K inhibitor 3-methyladenin during transient 2b expression in *N.*

198   *benthamiana* (15). The marked accumulation of the CMV RNA silencing suppressor 2b in *atg5*

199   (Fig 1E) supported this notion that 2b can be degraded by autophagy. Additionally, we also

200   found 2b accumulation in the *atg7* mutant compared to WT (Fig 4A). To further support 2b by

201   autophagy, we performed a GFP-based immunoprecipitation of GFP-ATG8a from mock and

202   CMV infected plants. We found that 2b, but also viral CP, co-purified with GFP-ATG8a (Fig

203   4B), suggesting both proteins may be degraded by autophagy during infection.

204   We further sought to analyse the autophagy-dependent targeting of 2b outside the

205   infection context. We found only a minor stabilization of 2b by conA in transgenic 2b seedlings

206   (Figure 4C), while NBR1 accumulated to substantial amounts, thus verifying the successful

207   inhibitor treatment. We speculated that either the rate of 2b autophagic degradation is slower

208   than that of NBR1 or the stability of these proteins differ in the vacuole. Nonetheless, after

209   introgression of the 2b transgene into the *atg5* background, we found much stronger

210   accumulation of 2b in *atg5* compared to WT (Fig 4D). Notably, NBR1 accumulated to higher

211   levels in WT plants expressing 2b, further supporting 2b-mediated reduction of autophagy. We

212   also noticed that the relative decrease in rosette biomass caused by 2b was much higher in *atg5*

213   plants compared to WT (Fig 4E), which could be a consequence of higher 2b levels, as 2b was

214   shown to facilitate virulence in a concentration-dependent manner (19), and increased

215   sensitivity of *atg5* to 2b virulence.

216   Finally, we carried out co-localization and immunoprecipitation experiments addressing

217   2b and CP association with ATG8a. 2b-RFP, but not CP-RFP, co-localized with GFP-ATG8a

218   in larger cytoplasmic structures (Fig 4F). 2b-RFP was also associated with multiple nuclear

219   speckles including the previously described targeting to the nucleolus (20), and caused re-

220   localization of GFP-ATG8a to the same domains (S1 Fig). CP-RFP also localized to the

221   nucleolus but without recruiting GFP-ATG8a. Interestingly, 2b re-localized CP-GFP but not

222   free GFP to the nuclear sub-compartments during their co-expression (S1 Fig). When 2b-RFP

223   and CP-RFP were co-expressed with either GFP or GFP-ATG8a followed by GFP-based

224   immunoprecipitation, we could detect specific association of 2b with ATG8a. An unspecific

225   signal arising from the RFP-antibody obscured judgement of co-purification of viral CP. Also,

226   no signal was detected in the purified samples using an antibody against CP (not shown), and

227   together with the absence of co-localisation between CP and ATG8a (Figure 4F), CP appears

228   not to be a prominent autophagy target, at least outside of infection. In conclusion, 2b protein

229   associates with ATG8a inside and outside of an infection context.

230

231   **Suppression of CMV RNA accumulation by autophagy involves AGO1 and Dicer proteins**

232   CMV 2b suppresses DCL2- and DCL4-dependent antiviral RNA silencing as shown by restored

233   pathogenicity of 2b-deficient CMV in the *dcl2 dcl4* knock-out mutant (21, 22). Furthermore,

234   2b interacts directly with AGO1 as part of RNA silencing suppression (23). We hypothesized

235   that autophagy could suppress CMV RNA accumulation by compromising 2b-dependent

236   suppression of RNA silencing. If this was the case, autophagy-dependent suppression of CMV

237   RNA accumulation should be less pronounced in *dcl2 dcl4* and *ago1* backgrounds. Indeed,

238   while CMV RNA accumulated to higher levels in both *atg7* and *dcl2 dcl4* mutants, there was

239   no additive effect in the *atg7 dcl2 dcl4* background at 14 DAI (Fig 5A). We obtained similar

240   results for AGO1 as the *ago1 atg5* double mutant did not show any additive increase in CMV

241   RNA accumulation compared to *atg5* and *ago1* single mutants (Fig 5B). The absence of

242   additive effects supports that autophagy and AGO1/DCL2,4-dependent resistance are coupled,

243   likely by autophagy targeting of the viral RNA silencing suppressor 2b.

244

Autophagy and RNA silencing synergistically support plant tolerance to CMV

246   Despite the apparent non-additive functions of autophagy and RNA silencing in reducing CMV

247   RNA accumulation at early stage of infection (Figure 5A and B), *atg7 dcl2 dcl4* mutants

248   eventually showed a total collapse when infections progressed further (Fig 5C). Notably, there

249   was no tissue senescence in either WT or *dcl2 dcl4* plants, while this autophagy-associated

250   phenotype was clearly visible in CMV-infected *atg7* and highly intensified in *atg7 dcl2 dcl4*

251   plants. When the fresh weight of the rosette was compared as a proxy of disease severity

252   between WT, *atg7*, *dcl2 dcl4* and *atg7 dcl2 dcl4* plants at 28 DAI, a strong additive effect on

253   biomass loss was observed in the combinatorial mutant of autophagy and RNA silencing (Fig

254   5D). We detected a similar dependence on biomass loss between *atg7* and *dcl2 dcl4* for the

255   unrelated dsDNA virus CaMV but not the RNA virus TuMV (S2 Fig). Possibly, TuMV fails to

256   show this dependence owing to very strong suppression of RNA silencing, as biomass loss was

257   overall highest for TuMV and comparable between WT and *dcl2 dcl4* in contrast to CaMV and

258   CMV. The severe biomass loss during CMV infection in the *atg7 dcl2 dcl4* mutants was further

259   corroborated by the loss of chlorophyll (Fig 5E). Because of the severe disease phenotype at 28

260   DAI, we chose to analyse the amount of viral 2b protein per plant as a measure of virus

261   accumulation instead of RT-qPCR. 2b accumulated to clearly higher levels in the single mutants

262   compared to WT (Fig 5F). 2b accumulated to higher levels also in the triple mutant compared

263   to WT when related to the loading control, but whether there are additive effects between *atg7*

264   and *dcl2 dcl4* remained unclear. These results suggested that impaired resistance could

265   contribute to the severe disease phenotype in the *atg7* and *dcl2 dcl4* mutants, and we speculate

266   that the escalated disease phenotype in the triple mutant may be a combination of the failure to

267   undergo partial recovery in *dcl2 dcl4* and enhanced virulence sensitivity in *atg7*.

268

269   **Autophagy is essential for transmission of CMV through seeds**

270   CMV belongs to those plant viruses that also transmit trans-generationally through seeds in a

271   process termed as vertical transmission. Vertical transmission is correlated with plant fecundity,

272   which we found to be substantially more reduced in autophagy-deficient *atg7* compared with

273   WT plants (Fig 6A). Interestingly, CMV infected *dcl2 dcl4* plants failed to produce seeds.

274   Despite reduced fecundity, the seed germination potential remained comparable between *atg7*

275   and WT irrespective of CMV infection (Fig 6B). Finally, we estimated CMV seed transmission

276   in offspring seedlings from infected WT and *atg7* plants. In WT plants, CMV showed a

277   transmission frequency of $1.31 \pm 0.8\%$ when calculated using Gibbs and Gower formulae (Fig

278   6C). This frequency of seed transmission is in the same range that has been reported for other

279   CMV strains in Arabidopsis (24). Notably, we did not detect any seed transmission in *atg7*

280   plants, establishing autophagy as essential for vertical transmission of CMV strain PV0187 in

281   Arabidopsis.

282

283

284 **DISCUSSION**

285 Autophagy can deliver a wide array of substrates including proteins, RNAs, ribosomes,

286 proteasomes, viral particles, organelles and aggregates for degradation in the lytic vacuole (1).

287 Hence, it plays an important role in maintaining plant homeostasis, especially when plants

288 encounter stressful conditions such as viral infections (25). The complexity of substrates

289 targeted by autophagy underscore the possibility that several distinct autophagic processes

290 operate in parallel upon cellular reprogramming and adaption to new conditions. This is

291 fortified by e.g. the uncoupling of autophagy-based plant virus resistance and tolerance against

292 TuMV (7), CaMV (8) and as demonstrated by this study, also CMV. The interaction between

293 CMV and autophagy is complex. It includes resistance and disease attenuation that is coupled

294 to RNA silencing components DCL2/DCL4 and AGO1 as well as autophagy-based degradation

295 of the major virulence factor 2b. Interestingly, 2b alone reduces plant growth in an autophagy-

296 dependent manner and shows a moderate capacity to dampen the autophagy response. The most

297 striking phenotype is the severely increased virulence of CMV during autophagy deficiency

298 that results in reduced plant life span, seed production and vertical virus transmission. Taken

299 together, these multiple connections between autophagy and infection emphasise the

300 complexity of this interaction in CMV epidemiology.

301   Plants reduce pathogen virulence by tolerance and resistance mechanisms, which are

302 assumed to impose different selective pressures on both pathogens and hosts (26). In this study

303 we found that autophagy contributes to the resistance against CMV by reducing virus

304 accumulation. While autophagy-mediated resistance has been established for several animal

305 viruses (12), comparative findings were largely lacking for plant viruses. Only very recently

306 we and others have found that autophagy targets multiple plant viruses, including the positive-

13

307   stranded RNA viruses TuMV and Barley stripe mosaic virus (7, 14, 27), the negative-stranded

308   RNA virus Rice stripe virus (13), the double-stranded DNA virus CaMV (8) and three single-

309   stranded DNA geminiviruses (9). These findings established autophagy as a central component

310   of plant immunity against viruses, which is fortified further by our current results on CMV.

311   Notably, these studies have revealed a wide mechanistic diversity of autophagy-based virus

312   resistance and viral counter-strategies (25), which ultimately suggests that different plant

313   viruses have co-evolved with the autophagy pathway in an individual manner. However, despite

314   the profound mechanistic differences in the detailed interaction between individual viruses and

315   autophagy, a common theme arising is the involvement of the RNA silencing pathway in the

316   autophagy-virus interplay (25). This connection is evident for CMV as we show that autophagy

317   degrades the viral silencing suppressor 2b and that the enhancement of viral RNA accumulation

318   in autophagy- and RNA silencing-deficient plants lack epistasis. These findings suggest that

319   autophagy-based CMV resistance requires a functional RNA silencing pathway, and we

320   speculate that this is causally linked to the degradation of the viral silencing suppressor 2b.

321   Notably, 2b is a highly complex pathogenicity factor that among other functions interacts with

322   AGO1/4 to impair slicing and also binds siRNAs directly (20, 23, 28, 29). Previously we

323   showed that the TuMV silencing suppressor HCpro is degraded by autophagy, also resulting in

324   reduced virus accumulation (7). Intriguingly, this effect appears to include the degradation of

325   potyvirus-induced structures reminiscent of RNA granules to which also AGO1 localizes (30).

326   Together with the autophagic degradation of the geminiviral satellite ßC1 silencing suppressor

327   (9), autophagy appears to be more generally nested into the antiviral RNA silencing defense

328   with virus-specific adaptations. Opposite to these antiviral roles of autophagy, viral proteins

329   have also been proposed to utilize autophagy for degrading the RNA silencing components

330   SGS3 and AGO1 (16, 17). Taking this into account, we need to consider that autophagy could

331   degrade 2b alone but also in complex with siRNA, AGO1 and other components. At least for

332   HCpro, autophagy seems to target higher-order RNA-protein complexes reminiscent of virus-

333   induced RNA stress granules and processing bodies (7, 30) with likely complex consequences

334   on infection. Whether viral proteins have evolved to function as autophagy cargo receptors to

335   mediate degradation of RNA silencing components is indeed an exciting option. Our results,

336   however, do not support that 2b uses this strategy to counteract RNA silencing-dependent

337   resistance, and in general autophagy seems to support rather than antagonize resistance against

338   plant viruses (7-9, 13, 14, 27).

339   Perhaps the most striking observation in the context of CMV and other viral infections

340   is the escalated disease severity in autophagy-deficient plants (Fig 5). It is likely that elevated

341   2b levels contributes to this phenotype as 2b virulence is dose-dependent (19) and accordingly

342   the growth of 2b transgenic *atg5* is severely reduced compared to 2b transgenic control plants

343   (Fig 4). Defects in RNA silencing alone also increase CMV virulence, but when combined with

344   autophagy deficiency the virulence intensifies to the extent that plants collapse and thus

345   terminate infection. Theory suggests that under strict vertical transmission, virulence should be

346   negatively correlated with the transmission rate (31-33). This can be reasoned because viral

347   fitness is tightly linked to the reproductive success of the host (34). Evidently, optimized

348   virulence benefits virus epidemiology, where virus accumulation and virulence need to be

349   balanced with plant longevity and fecundity to promote both successful horizontal and vertical

350   virus transmission (24, 32, 35). Thus, as autophagy and RNA silencing enhance plant longevity,

351   fecundity and vertical transmission of CMV, the antiviral nature of these pathways in a more

352   holistic and epidemiological context becomes less clear. 2b of CMV subgroup I, including the

353   virulent strains PV0187 (this study) and FNY, but not the mild LS strain of subgroup II,

354   localizes to the nucleolus (20, 36). Interestingly, nucleolar 2b appears to promote virulence

355   uncoupled from virus accumulation and this virulence is furthermore dampened by the RNA

356   silencing pathway (36). This finding is similar to our observation in combined autophagy and

357   RNA silencing knockout mutants. In this context, it is notable that 2b re-localized ATG8a to

358   the nucleolus. Functions associated with nuclear and nucleolar localized LC3, the mammalian

359   homolog of ATG8, are still undefined (37), and so far ATG8 has not been reported in the

360   nucleolus of plants. Despite a potential connectivity between these events, whether 2b-

361   dependent virulence involves nucleolar ATG8 functions remains a matter of future study.

362   2b is a major virulence factor and RNA silencing suppressor of CMV (36) and the strong

363   penalty of super-virulence arising from autophagy- and RNA silencing-deficiency highlights

364   the importance for CMV to fine-tuning these interactions. One exciting possibility is that CMV

365   recruits the autophagy pathway to degrade 2b in a regulated manner to minimize the resistance

366   penalty and support long-term tolerance. At the plant level, virus infections are prolonged

367   processes and the absolute amount of virus can continue to increase for several weeks during

368   systemic infection. However, the active cellular infection cycle is assumed to be largely

369   completed within 24 hours for most plant viruses, including CMV (38). During this relatively

370   short period, CMV may benefit from dampening the autophagy response using 2b without any

371   long-term tolerance costs. It is also interesting that the infection frequency is elevated in

372   autophagy-deficient plants for CMV (Fig 1), TuMV and CaMV (7, 8). This suggests that

373   autophagy suppresses initiation of plant virus infections in general, manifesting the autophagy-

374   virus interaction as most decisive at the very early infection stage. Once the active stage of

375   infection ceases in a cell, the autophagy-mediated clean-up of virulence factors like 2b should

376   promote long-term tolerance and possibly even reduce co-infection competition from weaker

377   viruses that would benefit from high levels of 2b. In line with this, the CP of CMV was recently

378   proposed to destabilize 2b in a self-attenuation mechanism by which the virus achieves long-

379   term virulence reduction (39). At this point, we can only speculate if CP-mediated 2b

380   degradation involves autophagy, but it is interesting that both 2b and CP were present in GFP-

381   ATG8a co-immunoprecipitations from infected plants (Fig 4) and that both proteins localize to

16

382   the nucleolar virulence domain of 2b (S2 Fig) (36). Nevertheless, our results revealed the

383   autophagic degradation of 2b during transgenic expression in the absence of CP, showing that

384   CP is at least not strictly required in this process. Taken together, we provide a hypothetical

385   model of autophagy as a complex regulator of CMV infection that influences virus

386   accumulation, transmission and plant disease (Fig 7).

387

388

389

17

Materials and methods

Plant material and growth conditions

Wild-type (WT) plants were *Arabidopsis thaliana* ecotype Columbia (Col-0). Mutants *atg5-1*, *atg7-2*, *nbr1-2*, *ago1-27*, *dcl2 dcl4*, *atg7 dcl2 dcl4*, and the GFP-ATG8a transgenic line have been described previously (40-43). The *ago1-27 atg5-1* double mutant was generated by crossing. The transgenic line 2b3C was described previously (19), and used for crossing with GFP-ATG8a and the *atg5-1* background. Arabidopsis plants were grown on soil for infection experiments under short-day conditions (8/16-h light/dark cycles) in a growth cabinet, and *Nicotiana benthamiana* plants were cultivated for transient expression assays under long-day conditions (16/8-h light/dark cycles) in a growth room at 150 µE/m²s, 21°C, and 70% relative humidity, respectively.

DNA constructs

ATG3 and *ATG8a* as well as viral cistrons *2a, 2b, 3a* and *CP* were amplified using cDNA prepared from CMV infected plant total RNA as template and cloned into pENTRY-Topo. *ATG3* was further recombined into pGWB614, and viral proteins into pGWB660 (44). Expression constructs for GUS and GFP-ATG8a were described in (8) and pRD400::*FLUC* in (45). *ATG8a* was recombined into pMDC32:*RLUC* (6) and all binary vectors were transformed into *Agrobacterium* C58C1 for transient expression in *N. benthamiana* or transformation of Arabidopsis by the floral dip method.

CMV inoculation and quantification

The first true leaves of 3-week-old Arabidopsis plants were inoculated mechanically with sap prepared from *N. benthamiana* plants infected with the CMV strain PV0187 described in (46). Plants were sampled in biological replicates, each containing 3 individual plants from which

415 inoculated leaves were removed. For CMV RNA or plant transcript quantitation, total RNA

416 was isolated using the RNeasy Plant Mini Kit (Qiagen), and on-column DNA digestion was

417 performed with DNase I (Qiagen). First-strand cDNA was done using Maxima First Strand

418 cDNA Synthesis Kit (Thermo Fisher Scientific). Quantitative RT-PCR analysis (qPCR) was

419 performed with Maxima SYBR Green/Fluorescein qPCR Master Mix (Thermo Fisher

420 Scientific) using the CFX Connect™ Real-Time PCR detection system (BIO-RAD) with gene-

421 specific primers listed in Supplemental Table 1. Normalization was done using *PP2A*

422 (*AT1G69960*).

423

Fresh weight and chlorophyll analysis

425 Fresh weight refers to the areal rosette of Arabidopsis plants after infection or stable

426 transformation, and is presented as ratios to the respective mock or non-transformed plants. The

427 relative chlorophyll content of plants was determined as described before (8).

428

Confocal microscopy and inhibitor treatment

430 Live cell images were acquired from abaxial leaf epidermal cells using a Zeiss LSM 780

431 microscope. Excitation/detection parameters for GFP was 488 nm/490-552 nm. Inhibitor

432 treatment was carried out with 0.5 μM concanamycin A in $^1/_2$ MS 10 h before confocal analysis.

433 Confocal images were processed with ZEN (version 2011). Quantitation of GFP-ATG8a

434 labelled puncta was done using Image J (version 1.48v) software essentially as described in (7).

435

Immunoblot analysis

437 Proteins were extracted in 100 mM Tris pH 7.5 with 2% SDS, boiled for 5 min in Laemmli

438 sample buffer and cleared by centrifugation. The protein extracts were then separated by SDS-

439 PAGE, transferred to polyvinylidene difluoride (PVDF) membranes (Amersham, GE

440   Healthcare), blocked with 5% skimmed milk in PBS, and incubated with primary antibodies

441   anti-NBR1 (47), anti-2b (20), anti-CP (Bioreba Art.Nr. 160612), anti-GFP (Santa Cruz

442   Biotechnology; sc-9996) using 1:2000 dilution in PBS 0.1% Tween-20, and secondary

443   horseradish peroxidase-conjugated antibodies 1:10 000 in PBS 0.1% Tween-20 (Amersham,

444   GE Healthcare). The immunoreaction was developed using the ECL Prime kit (Amersham, GE

445   Healthcare) and detected in a LAS-3000 Luminescent Image Analyzer (Fujifilm, Fuji Photo

446   Film).

447

448   **Immunoprecipitation**

449   For immunoprecipitation, plant tissue was homogenized in 2 ml buffer (100 mM Tris pH8, 150

450   mM NaCl, 0.5% TX-100, protease inhibitor cocktail (Roche)) per gram of tissue. The lysate

451   was cleared at 4000 x g for 5 min at 4°C, filtered through two layers of miracloth and incubated

452   1h with anti-GFP μbeads according to manufacturer's instruction (Milteney) for infected

453   Arabidopsis tissue and GFP-agarose beads (Chromotech) for transiently expressing *N.*

454   *benthamiana* tissue. After washing 4 times with buffer, samples were eluted using 2x Laemmli

455   sample buffer and analyzed by immunoblotting.

456

457   **Analysis of fecundity, germination potential and vertical virus transmission**

458   Plants grown under long-day conditions were infected with CMV and allowed to set seeds. The

459   seed weight was recorded and the relative fecundity is presented as a ratio between seeds from

460   control and infected plants. Seed germination potential of offspring seeds was recorded after

461   calculating the percentage of germinated seeds on ½ MS plates supplemented with 1% sucrose.

462   For vertical transmission, 10 pools of 20 seedlings each were analysed by RT-PCR per parental

463   plant for presence of CMV. Probability of virus transmission by a single seed was calculated

464   by the Gibbs and Gower's formulae (48) $p = 1 - \left(1 - \frac{y}{n}\right)^{1/k}$; where p is the probability of

465 virus transmission by a single seed, y is the number of positive samples, n denotes the total

466 number of samples assayed and k represents the number of seedlings taken per sample.

467

468 **Data analysis and presentation**

469 Data are presented as mean ± standard deviation (SD) and statistical significance was analyzed

470 by two-sided Student´s t-test with p-values <0.05 denoted * and p-values <0.01 denoted **.

471 The number of replicates is given in the respective figure legends (n).

472

473

474 **Acknowledgements**

475 We gratefully acknowledge John Carr for providing the CMV PV0187 strain and 2b transgenic

476 lines as well as Thomas Canto for the 2b antibody.

477

478

479 **Reference**

480 1. Batoko H, Dagdas Y, Baluska F, Sirko A. Understanding and exploiting autophagy

481 signaling in plants. Essays in biochemistry. 2017;61(6):675-85.

482 2. Rogov V, Dotsch V, Johansen T, Kirkin V. Interactions between autophagy receptors

483 and ubiquitin-like proteins form the molecular basis for selective autophagy. Mol Cell.

484 2014;53(2):167-78.

485 3. Michaeli S, Galili G, Genschik P, Fernie AR, Avin-Wittenberg T. Autophagy in Plants--

486 What's New on the Menu? Trends Plant Sci. 2016;21(2):134-44.

487 4. Soto-Burgos J, Zhuang X, Jiang L, Bassham DC. Dynamics of Autophagosome

488 Formation. Plant physiology. 2018;176(1):219-29.

21

489   5.   Hofius D, Li L, Hafren A, Coll NS. Autophagy as an emerging arena for plant-pathogen

490   interactions. Current opinion in plant biology. 2017;38:117-23.

491   6.   Ustun S, Hafren A, Liu Q, Marshall RS, Minina EA, Bozhkov PV, et al. Bacteria Exploit

492   Autophagy for Proteasome Degradation and Enhanced Virulence in Plants. The Plant cell.

493   2018;30(3):668-85.

494   7.   Hafren A, Ustun S, Hochmuth A, Svenning S, Johansen T, Hofius D. Turnip Mosaic Virus

495   Counteracts Selective Autophagy of the Viral Silencing Suppressor HCpro. Plant physiology.

496   2018;176(1):649-62.

497   8.   Hafren A, Macia JL, Love AJ, Milner JJ, Drucker M, Hofius D. Selective autophagy limits

498   cauliflower mosaic virus infection by NBR1-mediated targeting of viral capsid protein and

499   particles. Proceedings of the National Academy of Sciences of the United States of America.

500   2017;114(10):E2026-E35.

501   9.   Haxim Y, Ismayil A, Jia Q, Wang Y, Zheng X, Chen T, et al. Autophagy functions as an

502   antiviral mechanism against geminiviruses in plants. Elife. 2017;6.

503   10.   Dagdas YF, Belhaj K, Maqbool A, Chaparro-Garcia A, Pandey P, Petre B, et al. An

504   effector of the Irish potato famine pathogen antagonizes a host autophagy cargo receptor.

505   Elife. 2016;5.

506   11.   Paudel DB, Sanfacon H. Exploring the Diversity of Mechanisms Associated With Plant

507   Tolerance to Virus Infection. Front Plant Sci. 2018;9:1575.

508   12.   Dong XN, Levine B. Autophagy and Viruses: Adversaries or Allies? J Innate Immun.

509   2013;5(5):480-93.

510   13.   Fu S, Xu Y, Li C, Li Y, Wu J, Zhou X. Rice Stripe Virus Interferes with S-acylation of

511   Remorin and Induces Its Autophagic Degradation to Facilitate Virus Infection. Mol Plant.

512   2018;11(2):269-87.

513   14.   Yang M, Zhang Y, Xie X, Yue N, Li J, Wang XB, et al. Barley stripe mosaic virus gammab

514   Protein Subverts Autophagy to Promote Viral Infection by Disrupting the ATG7-ATG8

515   Interaction. The Plant cell. 2018;30(7):1582-95.

516   15.   Nakahara KS, Masuta C, Yamada S, Shimura H, Kashihara Y, Wada TS, et al. Tobacco

517   calmodulin-like protein provides secondary defense by binding to and directing degradation

518   of virus RNA silencing suppressors. Proceedings of the National Academy of Sciences of the

519   United States of America. 2012;109(25):10113-8.

520   16.   Cheng X, Wang A. The Potyvirus Silencing Suppressor Protein VPg Mediates

521   Degradation of SGS3 via Ubiquitination and Autophagy Pathways. Journal of virology.

522   2017;91(1).

523   17.   Derrien B, Baumberger N, Schepetilnikov M, Viotti C, De Cillia J, Ziegler-Graff V, et al.

524   Degradation of the antiviral component ARGONAUTE1 by the autophagy pathway.

525   Proceedings of the National Academy of Sciences of the United States of America.

526   2012;109(39):15942-6.

527   18.   Han S, Wang Y, Zheng X, Jia Q, Zhao J, Bai F, et al. Cytoplastic Glyceraldehyde-3-

528   Phosphate Dehydrogenases Interact with ATG3 to Negatively Regulate Autophagy and

529   Immunity in Nicotiana benthamiana. The Plant cell. 2015;27(4):1316-31.

530   19.   Lewsey M, Robertson FC, Canto T, Palukaitis P, Carr JP. Selective targeting of miRNA-

531   regulated plant development by a viral counter-silencing protein. The Plant journal : for cell

532   and molecular biology. 2007;50(2):240-52.

533   20.   Gonzalez I, Martinez L, Rakitina DV, Lewsey MG, Atencio FA, Llave C, et al. Cucumber

534   mosaic virus 2b protein subcellular targets and interactions: their significance to RNA silencing

535   suppressor activity. Molecular plant-microbe interactions : MPMI. 2010;23(3):294-303.

23

536   21.   Diaz-Pendon JA, Li F, Li WX, Ding SW. Suppression of antiviral silencing by cucumber

537   mosaic virus 2b protein in Arabidopsis is associated with drastically reduced accumulation of

538   three classes of viral small interfering RNAs. The Plant cell. 2007;19(6):2053-63.

539   22.   Ziebell H, Carr JP. Effects of dicer-like endoribonucleases 2 and 4 on infection of

540   Arabidopsis thaliana by cucumber mosaic virus and a mutant virus lacking the 2b counter-

541   defence protein gene. The Journal of general virology. 2009;90(Pt 9):2288-92.

542   23.   Zhang X, Yuan YR, Pei Y, Lin SS, Tuschl T, Patel DJ, et al. Cucumber mosaic virus-encoded

543   2b suppressor inhibits Arabidopsis Argonaute1 cleavage activity to counter plant defense.

544   Genes & development. 2006;20(23):3255-68.

545   24.   Pagan I, Fraile A, Fernandez-Fueyo E, Montes N, Alonso-Blanco C, Garcia-Arenal F.

546   Arabidopsis thaliana as a model for the study of plant-virus co-evolution. Philos Trans R Soc

547   Lond B Biol Sci. 2010;365(1548):1983-95.

548   25.   Kushwaha NK, Hafren A, Hofius D. Autophagy-virus interplay in plants: from antiviral

549   recognition to proviral manipulation. Mol Plant Pathol. 2019;20(9):1211-6.

550   26.   Roy BA, Kirchner JW. Evolutionary dynamics of pathogen resistance and tolerance.

551   Evolution. 2000;54(1):51-63.

552   27.   Li F, Zhang C, Li Y, Wu G, Hou X, Zhou X, et al. Beclin1 restricts RNA virus infection in

553   plants through suppression and degradation of the viral polymerase. Nat Commun.

554   2018;9(1):1268.

555   28.   Zhao JH, Liu XL, Fang YY, Fang RX, Guo HS. CMV2b-Dependent Regulation of Host

556   Defense Pathways in the Context of Viral Infection. Viruses. 2018;10(11).

557   29.   Goto K, Kobori T, Kosaka Y, Natsuaki T, Masuta C. Characterization of silencing

558   suppressor 2b of cucumber mosaic virus based on examination of its small RNA-binding

559   abilities. Plant Cell Physiol. 2007;48(7):1050-60.

560   30.   Hafren A, Lohmus A, Makinen K. Formation of Potato Virus A-Induced RNA Granules

561   and Viral Translation Are Interrelated Processes Required for Optimal Virus Accumulation.

562   PLoS pathogens. 2015;11(12):e1005314.

563   31.   Elena SF, Agudelo-Romero P, Carrasco P, Codoner FM, Martin S, Torres-Barcelo C, et

564   al. Experimental evolution of plant RNA viruses. Heredity (Edinb). 2008;100(5):478-83.

565   32.   Lenski RE, May RM. The evolution of virulence in parasites and pathogens:

566   reconciliation between two competing hypotheses. J Theor Biol. 1994;169(3):253-65.

567   33.   Alizon S, Hurford A, Mideo N, Van Baalen M. Virulence evolution and the trade-off

568   hypothesis: history, current state of affairs and the future. J Evol Biol. 2009;22(2):245-59.

569   34.   Lipsitch M, Siller S, Nowak MA. The Evolution of Virulence in Pathogens with Vertical

570   and Horizontal Transmission. Evolution. 1996;50(5):1729-41.

571   35.   Stewart AD, Logsdon JM, Jr., Kelley SE. An empirical study of the evolution of virulence

572   under both horizontal and vertical transmission. Evolution. 2005;59(4):730-9.

573   36.   Du Z, Chen A, Chen W, Liao Q, Zhang H, Bao Y, et al. Nuclear-cytoplasmic partitioning

574   of cucumber mosaic virus protein 2b determines the balance between its roles as a virulence

575   determinant and an RNA-silencing suppressor. Journal of virology. 2014;88(10):5228-41.

576   37.   Kraft LJ, Manral P, Dowler J, Kenworthy AK. Nuclear LC3 Associates with Slowly

577   Diffusing Complexes that Survey the Nucleolus. Traffic. 2016;17(4):369-99.

578   38.   Gonda T, Symons R. Cucumber Mosaic Virus Replication in Cowpea Protoplasts: Time

579   Course of Virus, Coat Protein and RNA Synthesis. Journal of General Virology. 1979;45:723-

580   736.

581   39.   Zhang XP, Liu DS, Yan T, Fang XD, Dong K, Xu J, et al. Cucumber mosaic virus coat

582   protein modulates the accumulation of 2b protein and antiviral silencing that causes symptom

583   recovery in planta. PLoS pathogens. 2017;13(7):e1006522.

584   40.   Hofius D, Schultz-Larsen T, Joensen J, Tsitsigiannis DI, Petersen NH, Mattsson O, et al.

585   Autophagic components contribute to hypersensitive cell death in Arabidopsis. Cell.

586   2009;137(4):773-83.

587   41.   Yoshimoto K, Jikumaru Y, Kamiya Y, Kusano M, Consonni C, Panstruga R, et al.

588   Autophagy negatively regulates cell death by controlling NPR1-dependent salicylic acid

589   signaling during senescence and the innate immune response in Arabidopsis. The Plant cell.

590   2009;21(9):2914-27.

591   42.   Zhou J, Wang J, Cheng Y, Chi YJ, Fan B, Yu JQ, et al. NBR1-mediated selective autophagy

592   targets insoluble ubiquitinated protein aggregates in plant stress responses. PLoS genetics.

593   2013;9(1):e1003196.

594   43.   Munch D, Teh OK, Malinovsky FG, Liu Q, Vetukuri RR, El Kasmi F, et al. Retromer

595   contributes to immunity-associated cell death in Arabidopsis. The Plant cell. 2015;27(2):463-

596   79.

597   44.   Nakagawa T, Kurose T, Hino T, Tanaka K, Kawamukai M, Niwa Y, et al. Development of

598   series of gateway binary vectors, pGWBs, for realizing efficient construction of fusion genes

599   for plant transformation. Journal of bioscience and bioengineering. 2007;104(1):34-41.

600   45.   Eskelin K, Suntio T, Hyvarinen S, Hafren A, Makinen K. Renilla luciferase-based

601   quantitation of Potato virus A infection initiated with Agrobacterium infiltration of N.

602   benthamiana leaves. J Virol Methods. 2010;164(1-2):101-10.

603   46.   Groen SC, Jiang S, Murphy AM, Cunniffe NJ, Westwood JH, Davey MP, et al. Virus

604   Infection of Plants Alters Pollinator Preference: A Payback for Susceptible Hosts? PLoS

605   pathogens. 2016;12(8):e1005790.

606   47.   Svenning S, Lamark T, Krause K, Johansen T. Plant NBR1 is a selective autophagy

607   substrate and a functional hybrid of the mammalian autophagic adapters NBR1 and

608   p62/SQSTM1. Autophagy. 2011;7(9):993-1010.

609   48.   Gibbs, A. J.; Gower, J. C. 1960: The use of a multiple transfer method in plant virus

610   transmission studies—some statistical points arising from the analysis of resuhs. Annals of
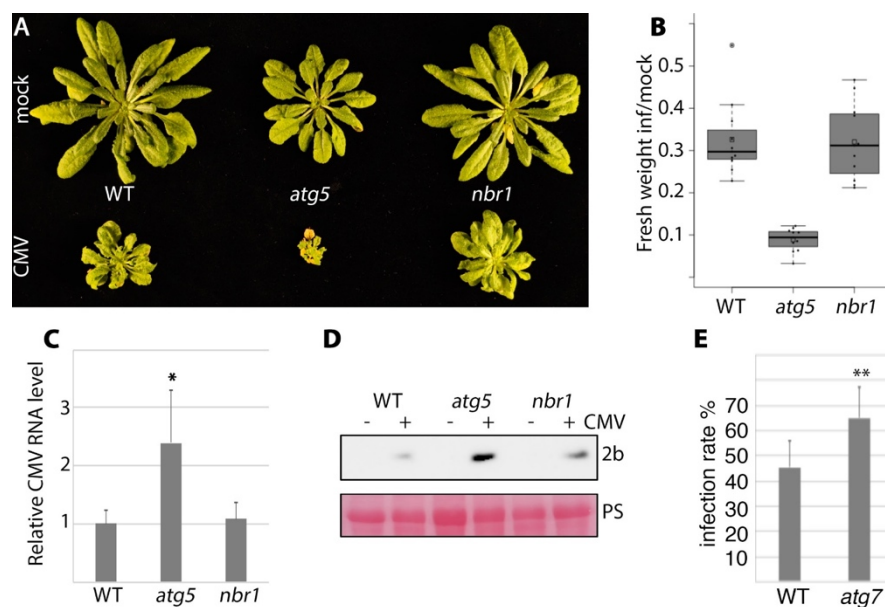
611   Applied Biology 48: 75-83.

612

613

Figures

Fig 1. Autophagy promotes plant tolerance and resistance against CMV infection

A) Representative WT (Col-0), *atg5* and *nbr1* plants at 28 days after mock or CMV inoculation.

B) The fresh weight ratio of CMV infected to mock plants 28 days after inoculation (DAI).

(*n*=9). C) Relative CMV RNA levels determined by RT-qPCR at 14 DAI. (*n*=4). D) In parallel

with (C), protein samples were prepared and CMV protein 2b was detected by Western blotting

using anti-2b. NBR1 detection was used to verify *atg5* and *nbr1* mutants and Rubisco large

subunit was visualized by Ponceau S staining (PS) of the membrane as loading control. E) CMV

infection rate in WT and *atg7* plants determined by presence/absence of viral symptoms three

weeks after mechanical sap inoculation. (*n*=8). Statistical significance (*$P<0.05$; **$P<0.01$)

was revealed by Student´s *t*-test (compared to WT).

629

630
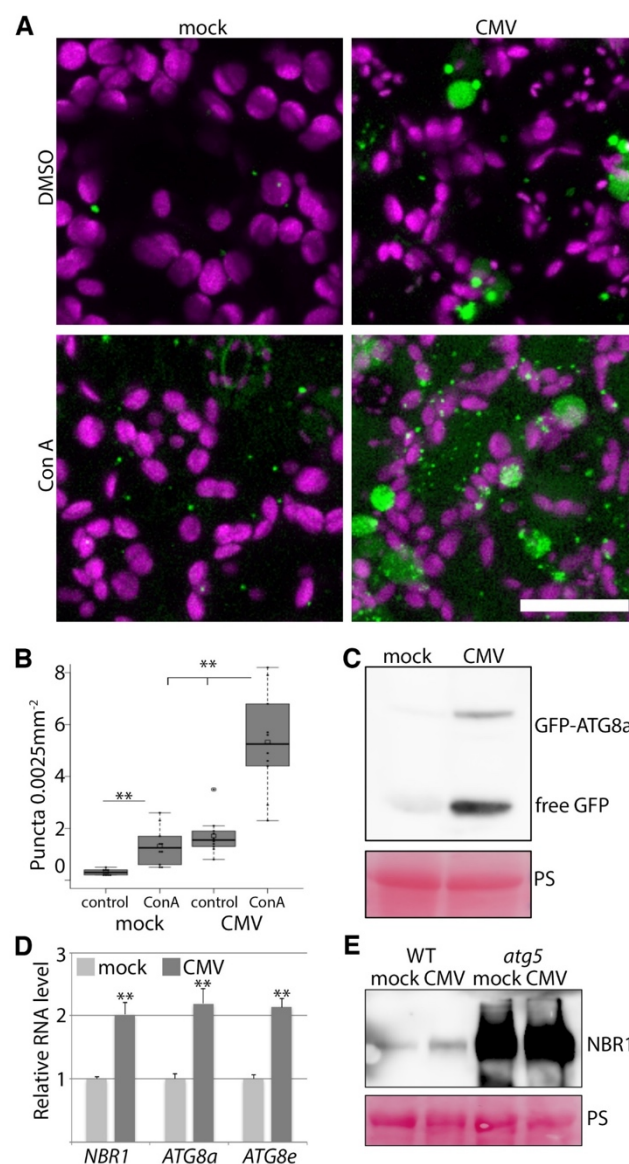
Fig 2. Autophagy is activated and functional during CMV infection

A) Representative images of the GFP-ATG8a marker in healthy and CMV infected plants

with and without concanamycin A (conA) treatment. Chloroplasts are shown in magenta.

Images are confocal Z-stacks. Scale bar = 20 μm. B) GFP-ATG8a foci were counted from

similar images as in (A) using Image J. (n=10). C) Western blot analysis of free GFP levels

derived from GFP-ATG8a in mock and CMV infected plants. Ponceau S (PS) staining

verified comparable protein loading. D) Transcript levels for *NBR1*, *ATG8a* and *ATG8e* in

mock and CMV infected plants were determined by RT-qPCR. (n=4). E) Western blot

29

639   detection of NBR1 levels in mock and CMV inoculated WT and *atg5* plants. Ponceau S (PS)

640   staining verified comparable protein loading. Statistical significance (*P<0.05; **P<0.01)

641   was revealed by Student´s *t*-test (compared to WT).

642

643
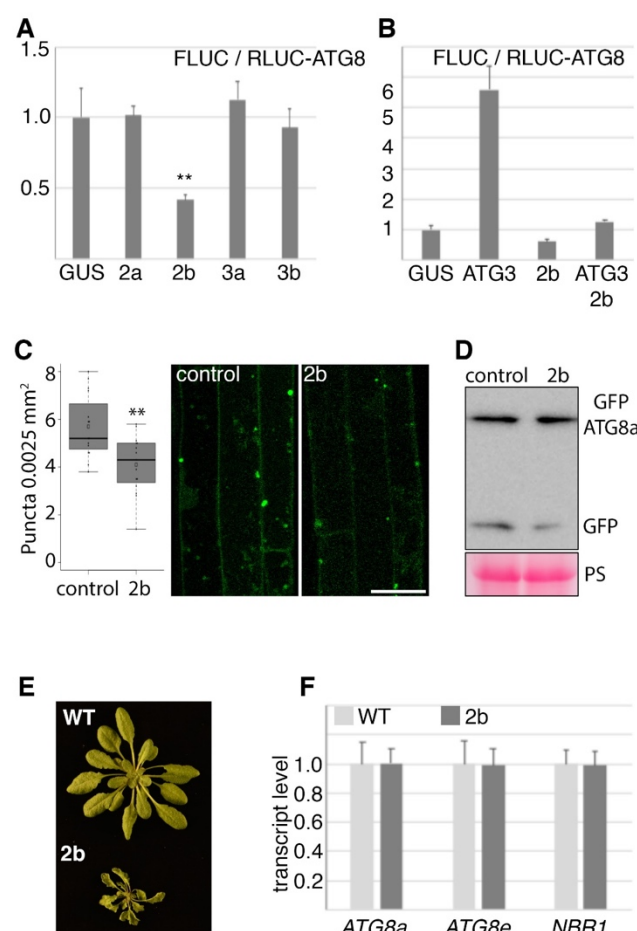
Fig 3. CMV protein 2b can dampen autophagy

A) RLUC-ATG8a and the internal control FLUC were co-expressed with viral proteins and GUS in leaves of *N. benthamiana*. Normalized luciferase values are given as a ratio between FLUC and RLUC, resulting in decreased ratios when RLUC-ATG8a degradation is reduced. (*n*=4). B) As in (A), but co-expressed proteins where GUS, ATG3, 2b and ATG3+2b. (*n*=4). C) The number of GFP-ATG8a foci were analyzed in roots of 10-day old seedlings without and with stable expression of 2b after 10h conA treatment. Counting was performed using ImageJ particle analyzer on confocal Z-stack projections. (*n*=15). Representative images are shown with scale bar = 20 μm. D) Anti-GFP western blot analysis was performed in parallel with (C) to estimate the ratio of GFP-ATG8a to free GFP. Rubisco large subunit visualized by Ponceau S staining (PS) of the membrane is shown as loading control. E) Representative image of 4-week-old short-day grown 2b expression line in comparison to WT plants. H) Transcript levels

31

656   of *ATG8a*, *ATG8e* and *NBR1* were determined by RT-qPCR using *PP2a* as reference from

657   plants shown in (E). (*n*=4). Statistical significance (**P<0.01) was revealed by Student´s *t*-test.
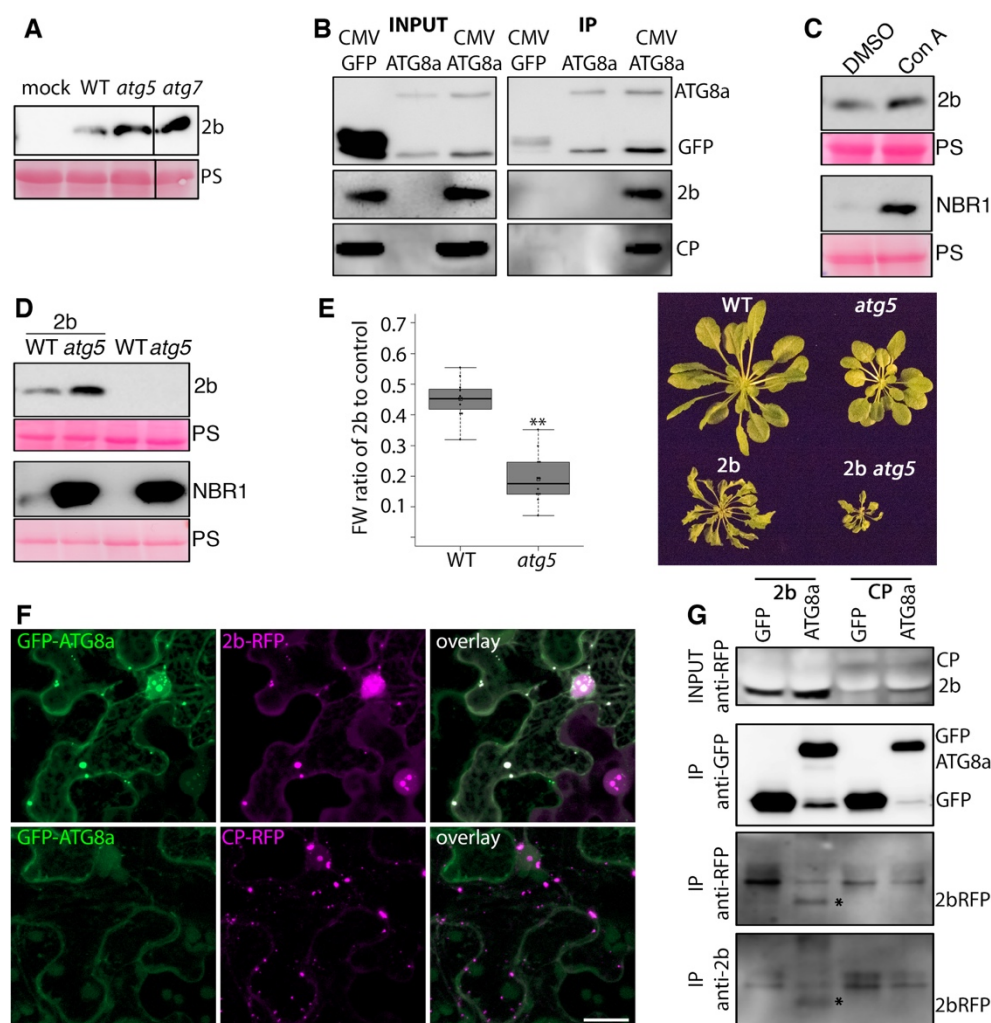
658

659

660

Fig 4. Autophagy degrades CMV 2b both in and outside the infection context

A) Accumulation of viral 2b protein was determined in WT, *atg5* and *atg7* plants at 14 DAI by western blot analysis. B) Co-immunoprecipitation analysis of viral CP and 2b with GFP-ATG8a from infected transgenic Arabidopsis tissue. Non-infected GFP-ATG8a and infected GFP expressing plants were used as control. Shown are the input and immunoprecipitated (IP) samples. C) 2b transgenic seedlings were treated with DMSO (control) or concanamycin A for 10h followed by western blot detection of 2b. Increased accumulation of NBR1 verified the concanamycin A (conA) treatment. D) Accumulation of 2b in transgenic WT and *atg5* plants was analyzed by western blotting. Increased accumulation of NBR1 verified the *atg5* background. Ponceau S-stained Rubisco shows loading (PS) in (A, C and D). E) 2b-dependent

671   virulence measured as relative fresh weight loss caused by transgenic 2b expression compared

672   to non-transgenic plants in WT and *atg5* backgrounds. (*n*=9). A representative plant image is

673   shown to the right. F) Co-localization analysis in *N. benthamiana* leaves co-expressing 2b-RFP

674   or CP-RFP with GFP-ATG8a. These Z-stack images were acquired 48 h post agroinfiltration.

675   Scale bar = 20 μm. G) Co-precipitation analysis of 2b-RFP and CP-RFP with GFP-ATG8a in

676   parallel with (F). Expression of GFP was used as control. Shown is the anti-RFP input signal,

677   as well as anti-GFP, anti-RFP and anti-2b signals from the GFP-based immunoprecipitated

678   samples. The position of 2b-RFP is marked with an asterisk.

679

680

681

682

683

684
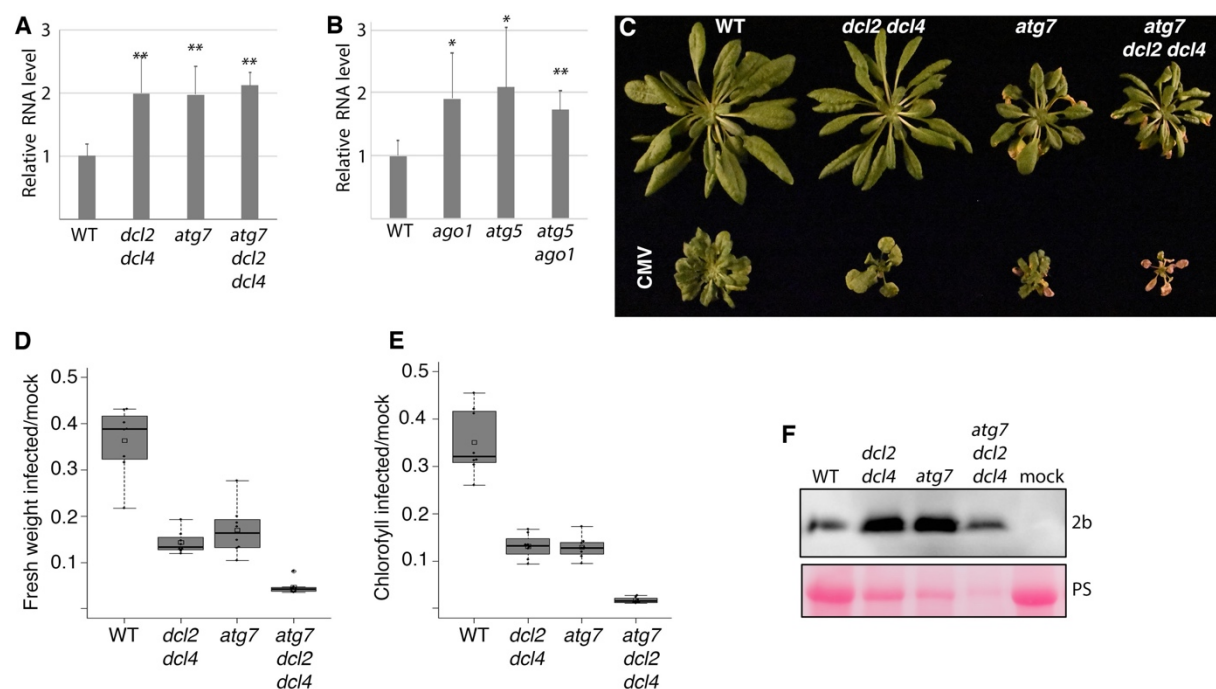
Fig 5. Autophagy-enhanced CMV resistance and tolerance are uncoupled and involve RNA silencing.

A) Relative CMV RNA levels determined by RT-qPCR at 14 DAI in WT, *atg7*, *dcl2 dcl4* and *atg7 dcl2 dcl4* plants (*n*=4). B) Relative CMV RNA levels determined by RT-qPCR at 14 DAI in WT, *atg5*, *ago1* and *atg5 ago1* plants (*n*=4). C) Representative image of mock-and CMV inoculated plants at 28 DAI. D and E) Relative fresh weight (D) and chlorophyll content (E) in CMV infected plants compared to mock at 28 DAI. (*n*=10). F) Western blot analysis of CMV 2b protein accumulation per plant in parallel with (C, D, E). Ponceau S stained Rubisco shows loading (PS) and reveals reduced total protein content per plant in the mutants compared WT.
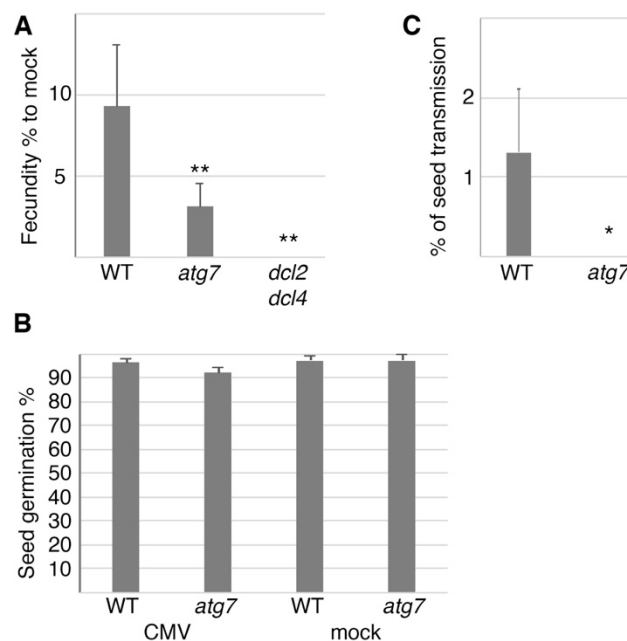
695

696

697

698

Fig 6. Autophagy and RNA silencing is essential for vertical transmission of CMV

A) Total seed weight of infected WT, *atg7* and *dcl2 dcl4* plants presented as a percentage

relative to seeds produced by non-infected mock plants. (*n*=5). B) The percentage of seeds

germinating from infected and non-infected WT and *atg7* plants. (*n*=5). C) Vertical

transmission of CMV was estimated by RT-PCR in seedlings derived from seeds of infected

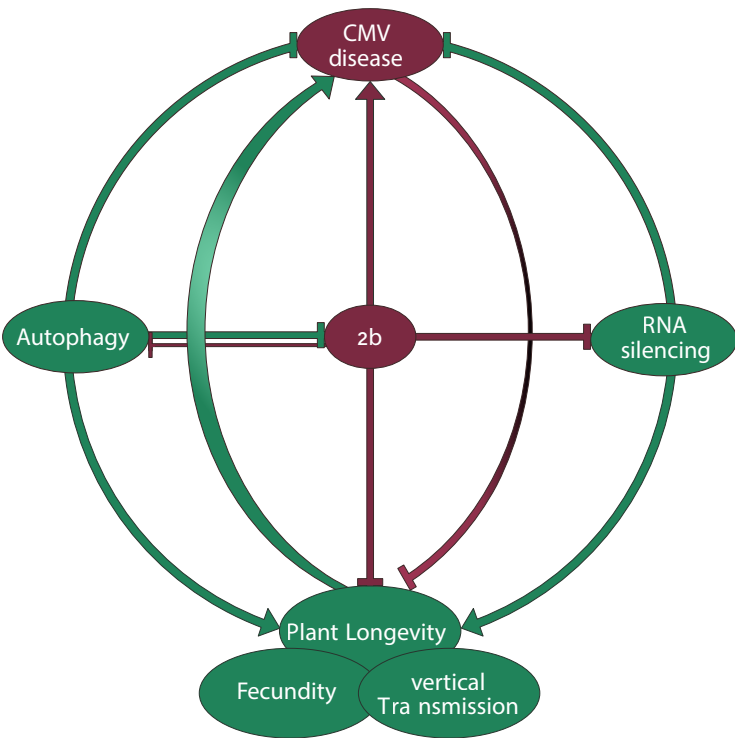WT and *atg7* plants (*n*=5 independent plants).

705

706

707

708

**Fig 7. Interplay between autophagy, RNA silencing and 2b shape CMV disease.**

709

The 2b protein is the major pathogenicity determinant in CMV infection. Plant autophagy

710

suppresses CMV accumulation through 2b degradation. By limiting 2b levels, autophagy

711

relaxes 2b mediated suppression of antiviral RNA silencing and virulence. Vice versa, 2b itself

712

has the capacity to restrict the plant autophagy response, but its significance during infection

713

remains to be resolved. Both autophagy and antiviral RNA silencing suppress virus

714

accumulation, and the lack of additivity between the pathways suggests their strong interaction

715

in the process, potentially through 2b. Taken together with their prominent synergism in disease

716

attenuation, we propose that autophagy and RNA silencing-based plant tolerance is not

717

quantitatively coupled to virus accumulation and that the pathways rather operate in a parallel

718

manner to promote survival of infected plants. Virulence evolution and trade-offs are

719

complicated for pathogens that utilize both vertical and horizontal transmission. Autophagy and

720

RNA silencing promotes CMV vertical transmission and likely also vector-mediated horizontal

721

transmission through increased plant longevity with only minor fitness penalties on virus

722

37

723   accumulation. We consider that CMV has adapted to and benefits from these potential antiviral

724   pathways. Thus, the interplay between the viral 2b protein, plant autophagy and RNA silencing

725   pathways determines the delicate balance between virus accumulation, transmission and plant

726   fitness in CMV disease.

727

728

729
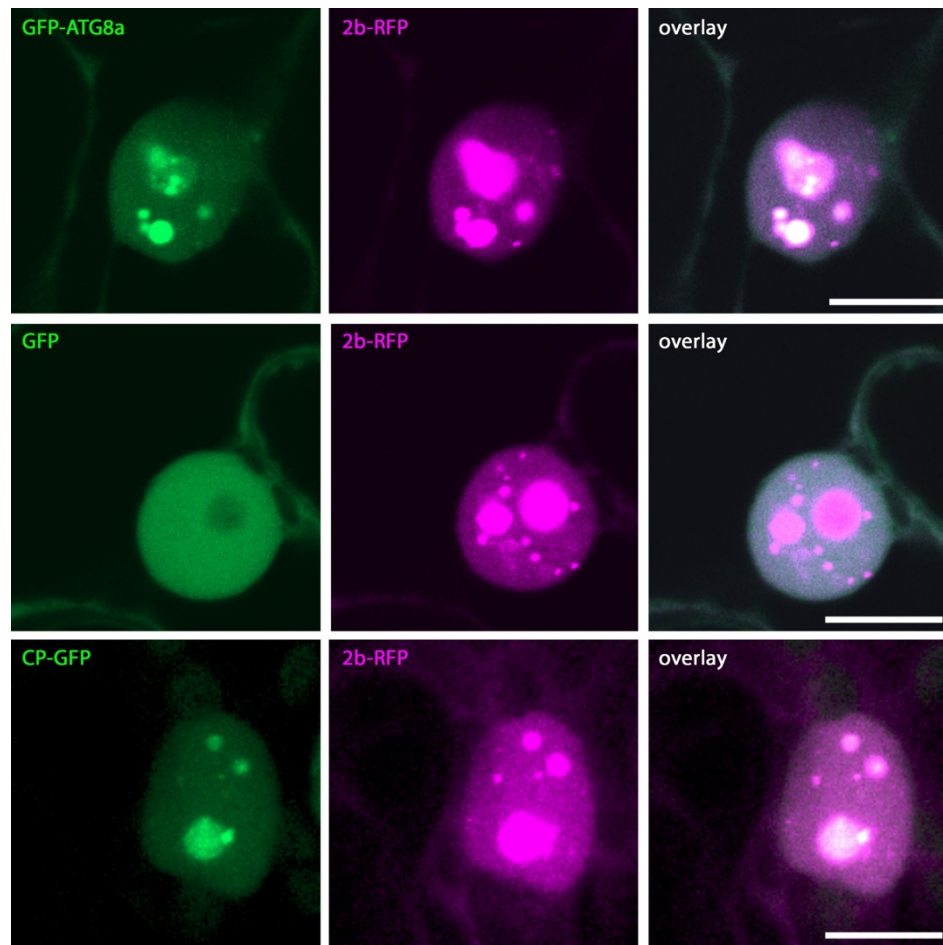
S1 Fig. Nuclear localization analysis of 2b-RFP, GFP-ATG8a, GFP and CP-GFP.

2b-RFP was co-expressed with GFP-ATG8a, GFP or CP-GFP in *N. benthamiana* and imaged

two days post agroinfiltration. GFP-ATG8a and GFP are single plains and CP-GFP a Z-stack

projection. Scale bar = 10 μm.

734

735

736

737
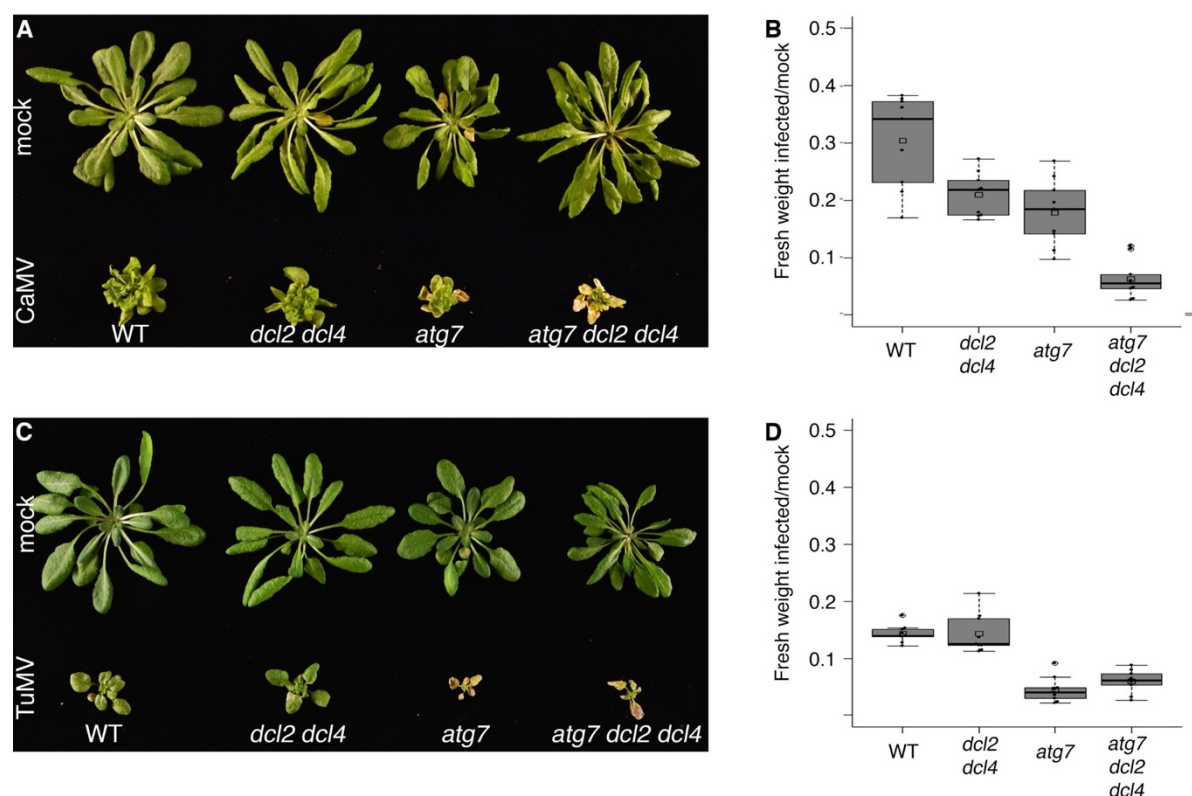
S2 Fig. RNA silencing and autophagy provide additive protection against CaMV but not

TuMV disease.

A) Representative image of mock and CaMV WT, *dcl2 dcl4*, *atg7* and *atg7 dcl2 dcl4* plants at

28 DAI. B) Fresh weight index representing the ratio between infected to mock plants. (*n*=9).

C) Representative image of mock and TuMV WT, *dcl2 dcl4*, *atg7* and *atg7 dcl2 dcl4* plants at

21 DAI. D) Fresh weight index representing the ratio between infected to mock plants. (*n*=9).

744

745

746

747

748

749